

Unitarity Corrections to the Proton Structure Functions at the Dipole Picture

M.B. Gay Ducati and M.V.T. Machado

*Instituto de Física, Univ. Federal do Rio Grande do Sul. Caixa Postal 15051,
91501-970 Porto Alegre, RS, BRAZIL.*

E-mail: gay@if.ufrgs.br, magnus@if.ufrgs.br

ABSTRACT: We study the dipole picture for the description of deep inelastic scattering, focusing on the structure functions which are driven directly by the gluon distribution. The current theoretical and phenomenological status are properly reviewed. One performs estimates using the effective dipole cross section given by the Glauber-Mueller approach in QCD, which encodes the corrections due to the unitarity effects associated with the saturation phenomenon. We also address issues about frame invariance of the calculations when analysing the observables.

KEYWORDS: Perturbative QCD calculations; Proton Structure Functions; Saturation Phenomenon.

1. Introduction

The scattering experiments on deep inelastic electron-proton (DIS) at HERA have provided measurements of the inclusive structure function $F_2(x, Q^2)$ as well as of the F_L and $F_2^{c\bar{c}}$ in very small Bjorken variable x ($x \ll 10^{-2}$). In these collisions the proton target is analysed through a hard probe with virtuality $Q^2 = -q^2$. The momentum fraction is $x \sim Q^2/2p \cdot q$, where p, q are the four-momenta of the incoming proton and the virtual photon probe. In such a kinematical region, the gluon is the leading parton driving the behavior of the deep inelastic observables. The standard QCD approach [1], whose technicality is now in good shape, reveals a powerlike growth for the gluon distribution and related quantities. This feature leads in principle to the unitarity violation at asymptotic energies. Thus, at high energies a taming of the gluon distribution increasing should be taken. In the partonic language, at the fast proton frame, the small momentum fraction region gives place to the high parton density domain. The latter is connected with the black disk limit of the proton target and with parton recombination phenomena. These issues can be addressed through a non-linear dynamics beyond the usual DGLAP formalism (for a review, see [2]). The complete knowledge about those dynamical regimes play an important role in the theoretical description of the reactions in the forthcoming experiments RHIC and LHC.

In the fast proton system, the QCD factorization theorem allows to calculate the scattering processes through the convolution of the partonic subprocess with the parton distribution functions (pdf's). There, the degrees of freedom of the theory are the quasi-free partons (quarks and gluons). On the other hand, most recently the theoretical description of the small x physics has been widely analyzed in the target rest frame, which is a powerful tool concerning an unified picture for both the inclusive and the diffractive scatterings, including vector meson production [3]. Now, the degrees of freedom are the color dipoles, which are the most simple configuration considering the virtual photon Fock states expansion. Its main appeal is a quite simplified picture for the different processes mentioned, based on general properties of quantum mechanics.

The description of DIS in the color dipole picture is quite intuitive, allowing a simple representation instead an involved one from the Breit (infinite momentum) frame. Such a framework was proposed by Gribov many years ago [4]. Considering small values of the Bjorken variable x , the virtual photon fluctuates into a $q\bar{q}$ pair (dipole) with fixed transverse separation r at large distances upstream of the target and interacts in a short time with the proton. More complicated configurations should be considered for larger transverse size systems, for instance the photon Fock state $q\bar{q} + \text{Gluon}$. An immediate consequence from the lifetime of the pair ($l_c = 1/2m_p x$) to be bigger than the interaction one is the factorization between the photon wavefunction and the cross section dipole-proton in the $\gamma^* p$ total cross sec-

tion. The wavefunctions are perturbatively calculable, namely through QED for the $q\bar{q}$ configuration [5] and from QCD for the $q\bar{q}G$ one [6]. Moreover, the effective dipole cross section should be modeled and encloses both perturbative and non-perturbative content. However, since the interaction strength relies only on the configuration of the interacting system the dipole cross section turn out to be universal and may be employed in a wide variety of small x processes [3].

Currently, there are several models for the dipole cross section based either in pure phenomenological parametrizations as in a most theoretical grounding (for a nice compilation, see Ref. [3]). The main feature in those models is the description of the energy dependence driving the interaction, namely taking into account the interplay between hard and soft domains. The dipole cross section should be consistent with the sharp growth on energy at small transverse separation r (large gluon density) and a softer behavior for larger r (Regge-like phenomenology). An additional ingredient is the expectation for saturation effects at high energies as a consequence of the unitarity requirements. Indeed, the growth of the gluon distribution should be tamed at very small x and it has been found that the corrections are important already in the present HERA kinematics [7]. Moreover, such effects are associated with higher twist contributions concerning the standard linear evolution equation, i.e. the DGLAP formalism [8].

Here, we take into account a well established formalism providing the unitarity corrections to the deep inelastic scattering at small x , namely the Glauber-Mueller approach in QCD. It was introduced by A. Mueller [9], who developed the Glauber formalism to study saturation effects in the quark and gluon distributions in the nucleus considering the academic case of heavy onium scattering. Afterwards, the authors of Ref. [10] extended that approach in lines of the GLR calculations [11]. There, in a most realistic way is constructed an evolution equation taking into account the unitarity corrections (perturbative shadowing), generating a non-linear dynamics which is connected with higher twist contributions. Its main characteristic is to provide a theoretical structure for the saturation effects, lying on the multiscattering of the pQCD Pomeron. The latter is represented through the usual gluonic ladder at double logarithmic approximation.

Summarizing the Glauber-Mueller approach, the gluonic content of the nucleus or nucleons is obtained in the following way. At the rest frame, a virtual probe (gluon) decays into a gluon pair interacting with the nucleon inside the nucleus. The multiple scatterings of the pair give rise to the unitarization of the corresponding cross section. The calculations are performed in the double logarithmic approximation (DLA), corresponding to the condition $\alpha_s \ll \gamma_G \ll 1$, where α_s and γ_G are the QCD coupling constant and the gluon anomalous dimension, respectively. In this approximation, the transverse separation of the pair remains fixed allowing an eikonal description for the interaction gluon pair-nucleon through incoherent multiscatterings [10]. The cross section for the interaction can be expressed in terms of

the nucleon gluon distribution $xG(x, \tilde{Q}^2)$ and of the transverse separation r of the gluon pair. The procedure for an initial state quark-antiquark pair is similar, up to proper color coefficients. Such a formulation has produced extensive phenomenological applications: the inclusive structure function F_2 [12], the longitudinal F_L and charmed $F_2^{c\bar{c}}$ ones [13], the logarithmic slope $\partial F_2/\partial \log Q^2$ [14] and another derivative quantities have been calculated in the Breit system. The respective nuclear case has been investigated in Refs. [15] and the equivalence with other high density QCD approaches has been reported at Refs. [16]. Moreover, the asymptotic limit of the inclusive structure function and its logarithmic slope are estimated at [17]. Regarding the rest frame, Glauber-Mueller has been also used to estimate saturation effects for DIS and diffractive dissociation [18] as well as it is considered as initial condition for a high energy evolution equation (see the pedagogical review [7]). Therefore, the Glauber-Mueller approach provides a good estimate for the unitarity effects (saturation) in the nucleon and nuclear sectors, constraining the dynamics of the observables in a quantitative level.

In this work we make use of the parton saturation formalism to study the description of the observables driven by the gluonic content of the proton at the color dipole picture. The saturation effects are included in the effective dipole cross section corresponding to the small size dipole contributions. The large dipole sizes are taken into account through the ansatz for the non-perturbative region. Here, we choose to freeze the gluon distribution at large distances. The dipole framework provides a clear identification in the transverse distance r range where the perturbative and non-perturbative sectors (soft domain) contribute to the calculated quantities. Indeed, the photon wavefunctions play a role of a weight function selecting small dipole sizes, however contributions coming from large dipole sizes are non-negligible. Moreover, when considering heavy quarks (charm and bottom), their masses also largely diminish the soft contribution. All these issues are addressed throughout this paper.

This work is organized as follows. In the next section we shortly review the deep inelastic at the rest frame, introducing the main formulae for the further analysis. In Sec. (3) one addresses the effective dipole cross section considering saturation effects (unitarity corrections) encoded in the Glauber-Mueller approach, pointing out its main properties and discussing the large transverse separation contribution. The Sec. (4) is devoted to calculate theoretical estimates for the HERA observables, focusing in those ones dominated by the gluon distribution. In the last section we draw our conclusions and comments.

2. The Deep Inelastic Scattering in the Proton Rest Frame

In the reference frame where the target (proton) has infinite momentum the usual description of the dynamics evolution is the following: the emitted partons from the target remain quasi-free enough time in such a way that the virtual probe (photon)

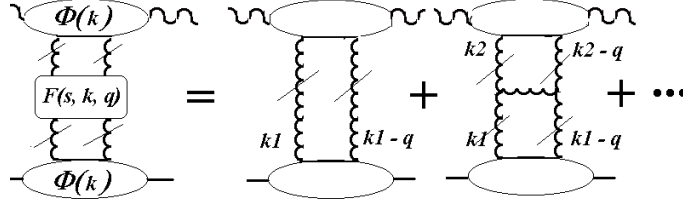


Figure 1: Representation of the deep inelastic process, where the upper blob corresponds to the photon impact factor and the bottom one represents the proton impact factor. The corresponding two first orders in perturbative expansion (BFKL-like) are depicted.

detects them as real particles (asymptotic freedom). On the other hand, in the small x region it is suitable to describe the evolution in a system where the target is at rest. In this situation, the evolution is related to the partonic fluctuations of the probe particle and their interactions with the nucleon. The rest frame physical picture is quite convenient since the lifetime of the photon fluctuation and the interaction process are well defined [19]. The simplest case is the quark-antiquark state (color dipole), which is the leading configuration for small transverse size systems. Its life time can be estimated by the uncertainty principle through the energy fluctuation associated with the emerging pair. The well known coherence length is expressed as $l_c = 1/(2xm_p)$, where x is the Bjorken variable and m_p the proton mass. For instance, in deep inelastic at HERA kinematics reaching at $x \sim 10^{-5}$, the coherence length is about 10^4 fm. This is a distance larger than the radius of any atomic nuclei. An immediate consequence of such a picture is the factorization between virtual photon wavefunctions and the interaction cross section on the corresponding amplitude in the impact parameter space representation (\mathbf{r}).

Looking at the momentum space representation, in the asymptotic high energy limit for photons with polarization δ , the deep inelastic cross section is written as [20]

$$\sigma_{\delta}^{\gamma^*p}(x, Q^2) = \frac{\mathcal{G}}{(2\pi)^4} \int \frac{d^2\mathbf{k}_1}{\mathbf{k}_1^2} \frac{d^2\mathbf{k}_2}{\mathbf{k}_2^2} \Phi_{\delta}^{\gamma^*}(\mathbf{k}_1) F(x, \mathbf{k}_1, \mathbf{k}_2) \Phi_p(\mathbf{k}_2) \quad (2.1)$$

Here, \mathcal{G} is the color factor for the color singlet exchange and \mathbf{k}_1 and \mathbf{k}_2 are the transverse momenta of the exchanged gluons in the t -channel [see Fig. (1)]. The $\Phi_{\delta}^{\gamma^*}(\mathbf{k}_2)$ is the virtual photon impact factor (with $\delta = T, L$) and $\Phi_p(\mathbf{k}_1)$ is the proton

impact factor. These quantities correspond to the upper and lower blobs in the Fig (1), respectively.

The impact factors $\Phi(\mathbf{k})$, describing the coupling between the interacting particles and the perturbative ladder are, by definition, factorized from the gluonic ladder $F(x, \mathbf{k}_1, \mathbf{k}_2)$. For instance, in the BFKL approach $F(x, \mathbf{k}_1, \mathbf{k}_2)$ is the Green's function for the Reggeon-Reggeon (= reggeized gluon) scattering. As a consequence, the energy dependence is determined by this function, remembering that the center of mass energy of the system $\gamma^* p$ is W^2 and that $x \approx Q^2/W^2$. The kernel $F(x, \mathbf{k}_1, \mathbf{k}_2)$ states the dynamics of the process, which is calculated in perturbative QCD and is independent of the external particles. It can encode the DGLAP formalism [1] as well as the BFKL approach [21] (or even the BFKL truncation [22]).

The diagrams at LO for the photon impact factor are well known, whereas they are not determined at NLO level of the perturbative expansion yet. However, recently it has been reported the effect of the exact kinematics of the exchanged gluons, which would give the most important contributions to the higher order terms [23]. This is quite important for a consistent calculation at NLO within the k_T -factorization framework. On the other hand, we are unable to compute the proton impact factor $\Phi_p(\mathbf{k}_1)$ using perturbation theory since it is determined by the large-scale nucleon dynamics and should be modeled [22]. In general, we can define a new quantity containing the perturbative kernel and the proton impact factor, named unintegrated gluon distribution:

$$\mathcal{F}(x, k) \equiv \frac{1}{(2\pi)^3} \int \frac{d^2k'}{k'^2} \Phi_p(k') k^2 F(x, k, k'), \quad (2.2)$$

where here we have avoided the bold representation for the two-dimensional vector \mathbf{k} . This quantity determines the probability of finding a gluon (or other parton) carrying the longitudinal momentum fraction x and transverse momentum \mathbf{k} . In principle, it should recover the conventional gluon (parton) density $G(x, Q^2)$ once the \mathbf{k} dependence is integrated out. Namely

$$\int_{\mu_0^2}^{\mu^2=Q^2} \frac{d^2\mathbf{k}}{\mathbf{k}^2} \mathcal{F}(x, \mathbf{k}) = x G(x, Q^2). \quad (2.3)$$

Recently, some procedures to determine the unintegrated gluon function directly or indirectly from data have been proposed. Quoting some of them, A.V. Lipatov et al. [24] have calculated a variety of vector meson production using BFKL-like phenomenological parametrizations for the function $\mathcal{F}(x, k_T)$. The charm structure function is also considered within the same procedure. In a most theoretical ground, Armesto and Braun [25] has obtained the unintegrated gluon (and quarks) function considering the scattering process mediated by fan diagrams of BFKL pomerons. The

results are employed to describe the nuclear structure functions and heavy flavours production.

Ivanov and Nikolaev [26] obtain a parametrization for $\mathcal{F}(x, Q^2)$ with a sophisticated matching between low and high transverse momentum (the transition scale is labeled k_c) and adding a soft contribution with x -independent behavior. The correspondence between k_T -factorization and DGLAP factorization is shown, addressing the issue of the contribution from the restricted part of the available transverse phase space in the leading $\log Q^2$ approximation.

On the other hand, Kimber et al. [27] proposed unintegrated distributions (including the quarks ones) depending on two hard scales $\mathcal{F}(x, k_T^2, \mu^2)$. From the fact that both DGLAP and BFKL evolutions are equivalent in the ordered evolution in the angles of the emitted gluons, the factorization scale μ^2 also controls the angular ordering of the gluon in the evolution. This fact allows obtain the unintegrated distribution from a single-scale evolution equation. Starting from the DGLAP formalism, $\ln(1/x)$ effects are included, and the scale μ^2 is introduced in the last step of the evolution. The latter is realized through the survival probability $T(k_T, \mu^2)$ that the gluon remains unaltered in the evolution up to scale μ .

Turning out, the deep inelastic cross section can be determined considering properly the photon impact factor and the unintegrated gluon distribution. Then Eq. (2.1) is written in the form,

$$\sigma_\delta^{\gamma^*p}(x, Q^2) = \frac{\mathcal{G}}{(2\pi)} \int \frac{d^2\mathbf{k}_1}{\mathbf{k}_1^4} \Phi_\delta^{\gamma^*}(\mathbf{k}_1) \mathcal{F}(x, \mathbf{k}_1). \quad (2.4)$$

For example, the impact factor for a photon longitudinally polarized is expressed as (see Ref. [20] for more details on the calculations)

$$\Phi_L(\mathbf{k}_1) = 16\alpha_{\text{em}}\alpha_s \sum_{i=1}^{n_f} e_i^2 \int dz \int d^2\mathbf{1} \left[Q^2 z^2 (1-z)^2 \left(\frac{1}{D_1} + \frac{1}{D_2} \right)^2 \right], \quad (2.5)$$

where α_{em} is the electromagnetic coupling and z is the longitudinal momentum fraction carried by the quark (having mass m_q). The notation $D_1 = \mathbf{1}^2 + \varepsilon^2$ and $D_2 = (\mathbf{1} - \mathbf{k}_1)^2 + \varepsilon^2$ is used, whereas $\varepsilon^2 = z(1-z)Q^2 + m_q^2$. The transverse contribution is obtained in a similar way [20].

Using the expressions for the corresponding impact factors, it arises a new representation for the cross section: it is determined from the partonic subprocess $\gamma^*g \rightarrow q\bar{q}$ (quark box), which is driven by perturbative QCD, and by the unintegrated gluon distribution. The latter one encodes all the non-perturbative content associated with the proton structure, but whose evolution is still determined by QCD. The factorization property verified in this case is denominated k_T factorization [28] and it is expressed as,

$$\sigma_\delta^{\gamma^*p}(x, Q^2) = \int \frac{dz}{z} \int \frac{d^2\mathbf{k}_1}{\mathbf{k}_1^2} \sigma_\delta^{\gamma^*g \rightarrow q\bar{q}}(z, Q^2, \mathbf{k}_1) \mathcal{F}\left(\frac{x}{z}, \mathbf{k}_1\right). \quad (2.6)$$

In the rest frame the most convenient description of the process is obtained in the impact parameter space representation, where the position of the partons in this space is frozen during the scattering. Therefore, we can rewrite the cross section (2.4) in terms of the impact parameter r through the Fourier transform, with \mathbf{r} being the conjugate variable to the transverse momentum \mathbf{k} [29].

For sake of illustration, the longitudinal photon impact factor (2.5) written in impact parameter space is expressed now as,

$$\Phi_L(\mathbf{k}_1) = 32\alpha_{\text{em}}\alpha_s \sum_{i=1}^{n_f} e_i^2 \int dz \int d^2\mathbf{r} (1 - e^{i\mathbf{k}_1 \cdot \mathbf{r}}) Q^2 z^2 (1-z)^2 K_0^2(\varepsilon r). \quad (2.7)$$

where $K_0(x)$ is the modified Bessel function of the second kind and order zero. The cross section for longitudinally polarized photons is straightforwardly obtained from Eq. (2.4),

$$\begin{aligned} \sigma_L^{\gamma^* p}(x, Q^2) &= \frac{6\mathcal{G}\alpha_{\text{em}}}{\pi^2} \sum_{i=1}^{n_f} e_i^2 \int dz \int d^2\mathbf{r} [Q^2 z^2 (1-z)^2 K_0^2(\varepsilon r)] \\ &\quad \times \left[\frac{4\pi\alpha_s}{3} \int \frac{d^2\mathbf{k}_1}{\mathbf{k}_1^4} \mathcal{F}\left(\frac{x}{z}, \mathbf{k}_1\right) (1 - e^{i\mathbf{k}_1 \cdot \mathbf{r}}) \right], \end{aligned} \quad (2.8)$$

A striking consequence of the formulation above is that the photoabsorption cross section can be derived from the expectation value of the interaction cross section for the multiparticle Fock states coming from the virtual photon over the light-cone wave functions of these states [5]. The scattering matrix has an exact diagonalization in the γ^* Fock states representation, where the partial-wave amplitudes subjected to the s -channel unitarization are identified properly. Then the photoabsorption cross section can be cast in the quantum mechanical form,

$$\sigma_{T,L}^{\gamma^* p}(x, Q^2) = \int d^2\mathbf{r} \int_0^1 dz |\Psi_{T,L}(z, \mathbf{r})|^2 \sigma^{\text{dipole}}(x, z, \mathbf{r}), \quad (2.9)$$

The formulation above is valid even beyond perturbation theory, since it is determined from the space-time structure of the process. The prompt identification is the $\Psi_{T,L}(z, \mathbf{r})$ being the photon wave function describing the pair configuration, where z and $1-z$ are the fraction of the photon's light-cone momentum carried by the quark and antiquark of the pair, respectively. The precise normalizations of the wavefunctions can be determined through the Fock expansion $|\gamma_{\text{phys}}\rangle = \sqrt{Z_3} |\gamma_{\text{bare}}\rangle + \mathcal{N}_{q\bar{q}} |q\bar{q}\rangle$, where Z_3 is the γ -wavefunction renormalization constant, $|\gamma_{\text{bare}}\rangle$ denotes the bare state and $\mathcal{N}_{q\bar{q}}$ is the coefficient determining the probability of the fluctuation $q\bar{q}$ pair in the photon [20]. Considering completely normalized states, then $\mathcal{N}_{q\bar{q}}^2 = 1 - Z_3$ and the normalization for transverse photons is obtained from $\int dz d^2\mathbf{r} |\Psi_{T,L}(z, \mathbf{r})|^2 = \mathcal{N}_{q\bar{q}}^2$. The remaining normalizations, i.e.

longitudinal component and cross section, are consequently fixed [20]. The explicit expressions are well known and one reads as,

$$|\Psi_T(z, \mathbf{r})|^2 = \frac{6\alpha_{\text{em}}}{4\pi^2} \sum_i^{n_f} e_i^2 \left\{ [z^2 + (1-z)^2] \varepsilon^2 K_1^2(\varepsilon r) + m_q^2 K_0^2(\varepsilon r) \right\} \quad (2.10)$$

and

$$|\Psi_L(z, \mathbf{r})|^2 = \frac{6\alpha_{\text{em}}}{4\pi^2} \sum_i^{n_f} e_i^2 \left\{ 4Q^2 z^2 (1-z)^2 K_0^2(\varepsilon r) \right\}. \quad (2.11)$$

Clarifying the notation, ε has been already defined with m_q the light quark mass, whereas K_0 and K_1 are the Mc Donald functions of rank zero and one, respectively.

The quantity $\sigma^{\text{dipole}}(x, z, \mathbf{r})$ is interpreted as the cross section of the scattering of the effective dipole with fixed transverse separation \mathbf{r} [5]. It is directly dependent on the unintegrated gluon distribution,

$$\sigma^{\text{dipole}}(x, z, \mathbf{r}) = \frac{4\pi\alpha_s}{3} \int \frac{d^2\mathbf{k}_1}{\mathbf{k}_1^4} \mathcal{F}\left(\frac{x}{z}, \mathbf{k}_1\right) (1 - e^{i\mathbf{k}_1 \cdot \mathbf{r}}) \quad (2.12)$$

The most important feature of the dipole cross section is its universal character, namely it depends only on the transverse separation \mathbf{r} of the color dipole. The dependence on the external probe particle, i.e. the photon virtuality, relies in the wavefunctions. Due to gauge invariance, the unintegrated gluon distribution vanishes at $|\mathbf{k}| \rightarrow 0$ (and similarly for the factor $(1 - e^{i\mathbf{k}_1 \cdot \mathbf{r}})$), and the dipole cross section has to be infrared finite.

2.1 The Phenomenological Dipole Cross Sections

The great technical difficulty in Eq. (2.12) is to model the unintegrated gluon distribution in a suitable way, mainly in the small transverse momentum (k_T) region (infrared sector). In particular, to obtain these distributions one should solve numerically an evolution equation [1,21,27], turning out the procedure cumbersome for practical use (instead, for a prompt parametrization see [26]). In general, this fact is headed off introducing an ansätze for the effective dipole cross section and analyzing the process in the impact parameter space. The main feature of the current models in the literature is to interpolate the physical regions of small transverse separations (QCD-parton improved model picture) and the large ones (Regge-soft picture).

Nevertheless, a closer connection of the dipole picture with the DGLAP formalism is far from clear yet. In the k_T -factorization framework, one can associate the standard parton distributions with the unintegrated ones through Eq. (2.3), at small dipole separation r (large transverse momenta $Q_0^2 \leq k_T \leq Q^2$) and at leading twist level. However, a sizeable amount of non-DGLAP contribution comes from the region $k_T \geq Q^2$ as pointed out in Ref. [26].

Recently, Munier et al. [30] (Munier-Staśto-Mueller, MSM) have determined in a model-independent way the dipole-proton cross section using data on diffractive electroproduction of vector mesons at HERA. The S -matrix element for the scattering, $S(x, \mathbf{r}, \mathbf{b})$, in particular the profile of the S -matrix is extracted considering the full t dependence for the process (b is the conjugate variable to momentum transfer t). It is stressed that the results depend weakly on the specific choice of the meson wavefunction.

$$\sigma_{\text{dipole}}^{\text{MSM}} = 2 \int d^2\mathbf{b} (1 - \mathcal{R}e S(x, \mathbf{r}, \mathbf{b})) . \quad (2.13)$$

The saturation scale Q_s^2 can be estimated using such a procedure and determining its dependence on the impact parameter b . Considering the phenomenological formula for the S -matrix, $S(x, r_Q, b) = \exp(-r_Q^2 Q_s^2(x, b)/4)$, it has been obtained $Q_s^2 = 1 - 1.5 \text{ GeV}^2$ for $b = 0.3 \text{ fm}$ and $Q_s^2 = 0.2 \text{ GeV}^2$ for $b = 1.0 \text{ fm}$. This work corroborates the reliability of the eikonal (Glauber-like) models and suggests the onset of unitarity effects at HERA, since the saturation scale lies in semihard values at small impact parameters.

The Manchester Group [31] proposed a parametric form which assumes two distinct terms carrying a Regge-like energy dependence (s either than $x \approx Q^2/s$). The hard term dominates at small r and vanishes as $r \rightarrow 0$. The soft one dominates at large r (it saturates) and has a almost flat behavior on energy.

$$\sigma^{\text{dipole}}(s, r) = H_{\text{soft}}(a_n^S, r) (r^2 s)^{\lambda_S} + H_{\text{hard}}(a_n^H, r) \exp(-\nu_H r) (r^2 s)^{\lambda_H} , \quad (2.14)$$

where $H_{\text{soft, hard}}$ are smooth polynomials in r with coefficients $a_n^{S, H}$. A successful fit to data determined the coefficients and the energy exponents $\lambda_{S, H}$, allowing to describe both electro and photoproduction at HERA as well as diffractive dissociation.

In similar lines matching soft and hard Pomeron, Donnachie and Dosh [32] construct in a proper formalism the dipole-dipole cross section. Using the Wilson loops technique, it is obtained in the form

$$\sigma_{\text{dipole}}(R_1, R_2) = \mathcal{N}_{\text{dip}} R_1 \left(1 - e^{-\frac{R_1}{3.1a}}\right) R_2 \left(1 - e^{-\frac{R_2}{3.1a}}\right) \quad (2.15)$$

where R_1 and R_2 are the transverse extensions of the light-like Wilson loops. The normalization is $\mathcal{N}_{\text{dip}} = \frac{0.67}{4\pi^2} [\langle g^2 FF \rangle a^4]^2$, where $\langle g^2 FF \rangle$ is the gluon condensate in a pure gauge theory and a is the correlation length of a gauge-invariant two-gluon correlator. The large dipoles couple to the soft pomeron and small ones couple to the hard pomeron. The model is in agreement with a variety of observables in photon-proton and photon-photon reactions [32].

The very appealing and popular phenomenological saturation model of Golec-Biernat and Wüsthoff (hereafter GBW) proposes a very economical description of

DIS data [33]. The corresponding cross section interpolates between color transparency, i.e. $\sigma^{\text{dipole}} \sim r^2$ at small r , and constant cross section σ_0 at large r (confinement). Such a procedure ensures Q^2 -saturation, while parton saturation at low x is obtained with an eikonal-inspired shape for the dipole cross section,

$$\sigma^{\text{GW}}(x, r^2) = \sigma_0 \left(1 - e^{-r^2/R_{\text{sat}}^2(x)} \right), \quad (2.16)$$

$$R_{\text{sat}}^2(x) = 4 R_0^2(x) = \frac{4}{Q_0^2} \left(\frac{x}{x_0} \right)^\lambda,$$

where the parameters $\sigma_0 = 23.03$ mb, $x_0 = 3.04 \cdot 10^{-4}$ and $\lambda = 0.288$ are fitted to the HERA DIS inclusive data with $x < 10^{-2}$, whereas $Q_0^2 = 1$ GeV² sets the dimension. The x -dependent saturation radius $R_0^2(x)$ scales the pair separation r in the cross section and is associated with the mean separation between partons in the nucleon. This approach was used to describe diffractive dissociation in a parameter-free way, considering also the required $q\bar{q}G$ configuration. Some criticism to the GBW model, mainly concerning a better knowledge of parton (gluon) distribution at low r and its saturation at small x are postponed to the next section. The most of them can also to be found in Refs. [3, 18].

Our work in this paper is closer to the McDermott et al. one [34] (hereafter McDFGS), where perturbative QCD relates the dipole cross section to the leading logarithmic gluon distribution function in the proton, at LLA(Q^2) accuracy.

$$\sigma^{\text{McDFGS}} = \frac{\pi^2 \alpha_s(\tilde{Q}^2)}{3} r^2 x G(x, \tilde{Q}^2) \quad (2.17)$$

where the identification $\tilde{Q}^2 = Q^2$ is allowed at leading-log level. A quite refined study of the dipole cross section is carried for all transverse separations r in [34]. The small r region is ascribed by the usual gluon pdfs, evolving with the scale $\tilde{Q}^2 = 10/r^2$, while in large separations ($r_{\text{pion}} \geq 0.65$ fm) the dipole cross section is driven by pion-proton contribution with the typical soft energy behavior from the hadronic sector. Moreover, the taming of the parton density is implemented by hand starting at the critical transverse separation r_{crit} , stated when the dipole cross section reaches one half of its maximum value labeled by the pion-proton cross section. In connection with the present work, the Glauber-Mueller approach gives at the Born level the Eq. (2.17). Instead of using an ad hoc control of the gluon distribution, the Glauber-Mueller provides the corrections required by unitarity in an eikonal expansion. For the large r region, we choose to follow a similar procedure from the GBW model, namely saturating (r -independent constant value) the dipole cross section at this region.

Having defined the notation and reviewed the main properties settled by the rest frame representation of deep inelastic process, in the next section we address the well established unitarity corrections formalism contained in the Glauber-Mueller approach, that we will consider in the calculation of the structure functions.

3. The Glauber-Mueller Approach

The Glauber formalism concerns mainly to interactions in nuclei, allowing to calculate the amount of unitarity corrections to the nuclear cross section. However this approach can be extended to take into account the taming of the partonic densities (saturation) through the multiple scatterings. Below, we review shortly the main properties of the Glauber formalism in QCD, either in the nuclear case as its extension to the nucleon case. We indicate the original papers [10] for a complete presentation. Here, it should be stressed that we are using the terminology saturation effects meaning unitarity corrections to the observables. Indeed, the asymptotic calculations have produced an unified $\ln(1/x)$ pattern for the cross section and gluon function instead of a truly saturated one [17].

Since the small x limit is driven by gluonic interactions, we consider a virtual probe G^* with invariant mass Q^2 which decays into a gluon pair GG having a transverse separation \mathbf{r} and transverse momentum \mathbf{k} . Then, the pair interacts with the target through a gluonic ladder at fixed transverse separation. In lines of the discussion from the previous section, the photoabsorption cross section for the probe particle in terms of x and virtuality Q^2 in the nuclear case is

$$\sigma_{tot}^{G^*A}(x, Q^2) = \int d^2\mathbf{r} \int_0^1 dz |\Psi_{GG}(z, \mathbf{r}, Q^2)|^2 \sigma^{GG-\text{nucleus}}(x, z, \mathbf{r}), \quad (3.1)$$

where the variables have the same identification as in the $q\bar{q}$ pair discussion. The quantity Ψ_{GG} is the light-cone wavefunction for the gluon pair. The Glauber's multi-scattering theory utilizes the phase shift method to describe processes on high energy for an incident particle undergoing successive scatterings. These scatterings are coherent in an interaction of a hadronic fluctuation, i.e. quark or gluon pairs, with the nucleus. There are interference effects among them, generating a reduction in the nuclear cross section, $\sigma^{\text{nucleus}} < A \sigma^{\text{nucleon}}$. Instead, for full incoherent scatterings the expectation is the nuclear cross section equals to $A \sigma^{\text{nucleon}}$. The well known Glauber formula for the total cross section of a hadronic state with the nucleus is

$$\sigma_{tot}^{\text{nucleus}} = 2 \int d^2\mathbf{b} \left(1 - e^{-\frac{1}{2} \sigma^{\text{nucleon}} S_A(\mathbf{b})} \right), \quad (3.2)$$

where $S_A(\mathbf{b})$ is a profile function containing the dependence on the impact parameter \mathbf{b} , which is the conjugate variable to the momentum transfer t . It is related to the nucleon distribution inside the nucleus and encodes the information about the angular distribution of the scattering. We discuss its particular shape later on. The Eq. (3.1) is quite general and allows to describe the hadronic fluctuations of the photon or any virtual probe, as saw in the last section.

The Glauber formula can be connected with the Eikonal model, which is largely employed in calculations on the hadronic sector. Considering the scattering amplitude dependent in the usual Mandelstan variables s and t , now written in the impact

parameter representation \mathbf{b} ,

$$a(s, \mathbf{b}) \equiv \frac{1}{2\pi} \int d^2\mathbf{q} e^{-i\mathbf{q}\cdot\mathbf{b}} \mathcal{A}(s, t = -q^2). \quad (3.3)$$

the corresponding total and elastic cross sections (from Optical theorem) are rewritten in the impact parameter representation (\mathbf{b}) as

$$\sigma_{tot} = 4\pi \text{Im} \mathcal{A}(s, 0) = 2 \int d^2\mathbf{b} \text{Im} a(s, \mathbf{b}), \quad (3.4)$$

$$\sigma_{el} = \int d^2\mathbf{b} |a(s, \mathbf{b})|^2, \quad (3.5)$$

The most important property when treating the scattering in the impact parameter space is the simple structure for the unitarity constraint [10]. At fixed \mathbf{b} , the constraint can be expressed in the following way,

$$\sigma_{tot} = \sigma_{el} + \sigma_{inel}, \quad (3.6)$$

$$2 \text{Im} a(s, \mathbf{b}) = |a(s, \mathbf{b})|^2 + C_{in}(s, \mathbf{b}), \quad (3.7)$$

with $C_{in}(s, \mathbf{b})$ denoting the sum of contributions coming from all the inelastic channels. The constraint above has a simple solution. If the real part of the scattering amplitude vanishes at the high energy limit, corresponding to small x values, the solution is

$$a(s, \mathbf{b}) = i \left[1 - e^{-\frac{1}{2}\Omega(s, \mathbf{b})} \right], \quad (3.8)$$

$$\sigma_{tot} = 2 \int d^2\mathbf{b} \left[1 - e^{-\frac{1}{2}\Omega(s, \mathbf{b})} \right], \quad (3.9)$$

where Ω is labelled opacity, an arbitrary real function and it should be determined by a detailed model for the interaction. The opacity function has a simple physical interpretation, namely $e^{-\Omega}$ corresponds to the probability that no inelastic scatterings with the target occur. To realize the connection with the Glauber formalism, the opacity function can be written in the factorized form $\Omega(s, \mathbf{b}) = \Omega(s) S(\mathbf{b})$, considering $S(\mathbf{b})$ normalized as $\int d^2\mathbf{b} S(\mathbf{b}) = 1$ (for a detailed discussion, see i.e. [35]).

From Eqs. (3.9) and (3.2), we identify the opacity $\Omega(s \approx Q^2/x; \mathbf{r}) = \sigma^{\text{nucleon}}(x, \mathbf{r})$. Moreover, it has been found that the same formalism for multiple scatterings can be applied to the nucleon case. To proceed, we should determine the GG cross section. The gluon pair cross section is equivalent to the quark pair one, up to a color factor ($\sigma^{GG} = \frac{9}{4}\sigma^{q\bar{q}}$). The $(q\bar{q}$ pair) dipole-proton cross section is well known [10, 35], which is calculated starting from Eq. (2.12), and in double logarithmic approximation (DLA) has the following form

$$\sigma_{\text{nucleon}}^{q\bar{q}}(x, r) = \frac{\pi^2 \alpha_s(\tilde{Q}^2)}{3} r^2 x G(x, \tilde{Q}^2) \quad (3.10)$$

with the r -dependent scale $\tilde{Q}^2 = r_0^2/r^2$. Considering Eq. (3.10) one can connect directly the dipole picture with the usual parton distributions (gluon), since they are solutions of the DGLAP equations. In our case, we follow the calculations in Ref. [10,35] and consider the effective scale $\tilde{Q}^2 = 4/r^2$. Such a value differs from [34], where is $r_0^2 = 10$, which is obtained by an averaging procedure on the transverse size integral of F_L . However, in further studies in vector mesons it was found that r_0^2 ranges from 4-15 and F_2 and F_L are not sensitive to those variations. Thus, these values are consistent in leading logarithmic Q^2 approximation.

From the above expression, one obtains a dipole cross section satisfying the unitarity constraint and a framework to study the unitarity effects (saturation) in the gluon DGLAP distribution function. Hence, hereafter we use the Glauber-Mueller dipole cross section given by

$$\sigma_{\text{dipole}}^{GM} = 2 \int d^2\mathbf{b} \left(1 - e^{-\frac{1}{2} \sigma_{\text{nucleon}}^{\text{q}\bar{\text{q}}}(\mathbf{x},\mathbf{r}) S(\mathbf{b})} \right). \quad (3.11)$$

Here, some comments are in order. The Glauber-Mueller approach is valid at small x region, and the gluon emission is described in the double logarithmic approximation of the perturbative QCD. The interaction of the quark pair with the nucleon (proton) occurs through ladder diagrams exchange, satisfying the DGLAP equations at DLA limit. The high energy limit allows to treat successive scatterings as independent collisions, becoming the process described by the classic eikonal picture of a relativistic particle crossing the nucleus. Moreover, as a consequence of no correlation among nucleons inside the nucleus (in the nuclear case), implies no correlations among partons from different partonic cascades. It should be stressed that only the fastest partons interacts with the target. The corrections coming from the slowest partons in the cascade (emitted by the pair) lead to the AGL non-linear evolution equation [10]. They have been considered recently to describe diffractive DIS in Ref. [18]. Regarding criticisms to the Glauber-Mueller approach, we indicate the recent paper [36] for a complete discussion about the eikonal-like models, concerning their advantages and limitations as well as pointing out the improvements to be taken into account to introduce the proper corrections.

Now, we proceed to calculate numerical estimates of the dipole cross section using the Glauber-Mueller approach through Eqs. (3.10-3.11). Then we are calculating saturation effects in the color dipole picture. Firstly, we need to discuss the profile function $S(\mathbf{b})$. This function contains information about the angular distribution in the scattering, namely the t dependence (quark pair-ladder and proton-ladder couplings). Both of them can be approximated by an exponential parametrization, leading to a simple gaussian shape in the impact parameter space,

$$S(\mathbf{b}) = \frac{A}{\pi R_A^2} e^{-\frac{b^2}{R_A^2}}, \quad (3.12)$$

where A is the atomic number and R_A is the target size. The R_A^2 value should be determined from data on process scanning the angular dependence, in general ranging over $5 - 17 \text{ GeV}^{-2}$ for the proton case (see discussions in [7,18]). For nuclear reactions, a more sophisticated shape for the profile should be taken into account. Here, we have used the value ($R_A^2 = 5 \text{ GeV}^{-2}$) obtained from a good description of both inclusive structure function and its derivative [14]. Such a value corresponds to strong corrections to the standard DGLAP input.

Now, one discuss in a detailed way the main characteristics emerging from the dipole cross section Eq. (3.11). In this order, in Fig. (2) one shows the Glauber-Mueller dipole cross section as a function of dipole transverse size r at fixed momentum fraction x . For sake of a better illustration on the expected partonic saturation effects, we run the Bjorken x down to a quite small value $x = 10^{-7}$ (THERA region). Hereafter, we are using the GRV gluon distribution at leading order [37] in the input Eq. (3.10), whose choice we justify below. The solid lines correspond to the dipole cross section calculation, Eq. (3.11), whereas the dashed lines are the GBW model [33] depicted for sake of comparison. The general shape in terms of the dipole size comes from the balancing between the color transparency $\sigma_{dip} \sim r^2$ behavior and the gluon distribution shape.

Here some comments about the large transverse separation are in order. Although perturbative QCD provides us with reliable results at small distances (small dipole sizes), the nonperturbative sector is not still completely understood. The usual pdf's are evolved from a perturbative initial scale $Q_0^2 \approx 1 \text{ GeV}^2$, and one has little information about the behavior at $Q^2 \leq Q_0^2$. In general one makes use of Regge phenomenology to estimate those contributions (see, for instance [34]). Thus, extrapolating to lower virtuality regions (large dipole sizes) one needs an ansatz regarding the nonperturbative sector.

This is the main justification of the use the GRV94 parametrization [37] in our calculations. Bearing in mind that $Q^2 = 4/r^2$, its evolution initial scale is $Q_0^2 = 0.4 \text{ GeV}^2$ allowing to scan dipole sizes up to $r_{\text{cut}} = \frac{2}{Q_0} \text{ GeV}^{-1}$ ($= 0.62 \text{ fm}$). For the most recent parametrizations, where $Q_0^2 \sim 1 \text{ GeV}^2$ ($r_{\text{cut}} \approx 0.4 \text{ fm}$) the amount of nonperturbative contribution in the calculations it should increase. An additional advantage is that GRV94 does not include non-linear effects to the DGLAP evolution since the parametrization was obtained from rather large x values. This feature ensures that the parametrization does not include sensible unitarity corrections in the initial scale.

Now, we should introduce an ansatz for the large transverse separation region. A more phenomenological way is to match the pQCD dipole cross section with the typical hadronic one $\sigma_{\pi N}$ at r_{cut} as performed in [34]. However, due to the significative growth of the pQCD dipole cross section at high energies, we choose an alternative ansatz: the gluon distribution is frozen at scale r_{cut} , namely $x G(x, \tilde{Q}_{\text{cut}}^2)$. Then, for

the large distance contribution $r \leq r_{\text{cut}}$ the gluon distribution reads as,

$$x G(x, Q^2 \leq Q_0^2) = \frac{Q^2}{Q_0^2} x G(x, Q^2 = Q_0^2), \quad (3.13)$$

leading to the correct behavior $x G \sim Q^2$ as $Q^2 \rightarrow 0$. In a more sophisticated case, one can substitute the freezed scale \tilde{Q}_{cut}^2 for the saturation scale $Q_s^2(x)$ to take into account a realistic value of the gluon anomalous dimension in all kinematic region (see correlated issues in [18]).

Recently, the quite economical phenomenological model of Ref. [33] has produced a good description of HERA data in both inclusive and diffractive processes. It is constructed interplaying the color transparency behavior $\sigma_{dip} \sim r_{\perp}^2$ at small dipole sizes and a flat (saturated) behavior at large dipole sizes $\sigma_{dip} \sim \sigma_0$ (confinement). The expression has the eikonal-like form,

$$\sigma_{q\bar{q}}(x, r) = \sigma_0 \left[1 - \exp \left(- \frac{r^2 Q_0^2}{4(x/x_0)^\lambda} \right) \right], \quad (3.14)$$

where $Q_0^2 = 1 \text{ GeV}^2$ and the three fitted parameters are $\sigma_0 = 23.03 \text{ mb}$, $x_0 = 3.04 \cdot 10^{-4}$ and $\lambda = 0.288$ and the notation for the saturation radius $R_0(x) = (x/x_0)^{\lambda/2}$. The GBW dipole cross section lies below the typical hadronic cross section, namely $\sigma_{dip} \leq \sigma_{\pi N}$. Despite describing data in good agreement, GBW has some details that deserve certain discussion: the approach does not present a dynamical hypothesis for the saturation phenomena and does not match DGLAP evolution. In GBW, saturation is characterized by the x -dependent saturation radius $Q_s^2(x) = 1/R_0^2(x)$ instead of the most involved scale coming from Glauber-Mueller, $\kappa_G(x, Q_s^2) = 1$, which can be easily extended for the nuclear case.

In Fig. (2) one shows the Glauber-Mueller dipole cross section and the GBW model [33]. We choose to compare them due to the fact that GBW is actually a particular case of the Glauber-Mueller approach, considering an oversimplified profile function. We should show below that this fact allows construct an extended saturation model with DGLAP evolution [38] (BGK model). Following, in the lower plots, where $x = 10^{-3}$ and $x = 10^{-4}$, the GM cross section underestimates the GBW one. However, as x decreases the gluon distribution in the proton rises turning out the dipole cross section bigger. This feature is depicted in the upper plots, for smaller $x = 10^{-6}$ and $x = 10^{-7}$, where GM overestimates GBW by a significant factor mostly at intermediate r values. Thus, GM overestimates the typical hadronic cross sections at higher energies. For discussions about this question, see Ref. [34]. We disregard such a feature in our further analysis.

Finally, we show the connection between the Glauber-Mueller approach with the saturation model with DGLAP evolution [38]. Considering the particular case of central collisions, namely scattering at impact parameter $b = 0$ ($S(b) = A/\pi R_A^2$),

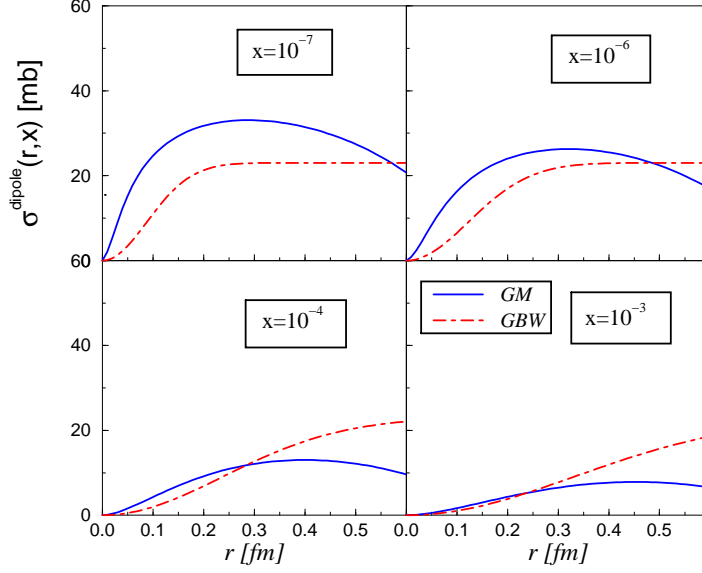


Figure 2: The dipole cross section as a function of r at fixed x . The Glauber-Mueller (GM) corresponds to the solid line and the GBW model results (dashed curves) are also included.

the Glauber-Mueller approach produces,

$$\sigma_{\text{dipole}}^{GM}(x, \mathbf{r}, b = 0) = 2 \int d^2\mathbf{b} \left(1 - e^{-\frac{1}{2} \sigma_{\text{nucleon}}^{q\bar{q}}(x, \mathbf{r}) \frac{1}{\pi R_A^2}} \right). \quad (3.15)$$

The integration over b can be promptly carried out, and introducing the notation for the proper normalization for the dipole cross section,

$$\sigma_0 \equiv 2\pi \int_0^{R_A^2} db^2 = 2\pi R_A^2, \quad (3.16)$$

the Eq. (3.15) recovers the simple expression for the saturation model DGLAP evolved [38],

$$\sigma_{\text{dipole}}^{BGK}(x, \mathbf{r}) = \sigma_0 \left(1 - e^{-\frac{\sigma^{q\bar{q}}(x, \tilde{Q}^2)}{\sigma_0(R_A^2)}} \right). \quad (3.17)$$

For a phenomenological analysis, the parameter σ_0 and the scale \tilde{Q}^2 are determined from data in [38]. In our case, it assumes the well defined values $\sigma_0 = 12.22$ mb [using $R_A^2 = 5 \text{ GeV}^{-2}$ in Eq. (3.16)] and our virtuality scale is $\tilde{Q}^2 = 4/r^2$. Instead, BGK choose the parametric form $\tilde{Q}^2 \equiv \mu^2 = C/r^2 + \mu_0^2$ and a two-parameter initial condition for the gluon distribution function. The matching between the saturation model and DGLAP evolution is timely, since it is quite efficient describing data and its qualitative success corroborates quantitative QCD studies.

4. Unitarity Effects in ep Collisions

This section is devoted to the study and estimate of the gluon driven observables measured at HERA kinematical domain in the rest frame. The first one is the inclusive structure function $F_2(x, Q^2)$, the main quantity testing the small x physics. The unitarity corrections are well established for this observable considering Glauber-Mueller approach [12] as well as its high energy asymptotics [17], namely the black disk limit. We review these issues considering the dipole picture (rest frame), using a more complete analysis similar to [33, 34]. We discuss in detail the role played by the nonperturbative physics needed to describe the structure function and where in the transverse separation r range it starts to be important.

The longitudinal structure function $F_L(x, Q^2)$ is also addressed, verifying the frame invariance in comparison with previous laboratory frame calculations [13]. The longitudinal wavefunction strongly suppress large r contributions, thus selecting smaller nonperturbative contribution in comparison with the F_2 case. Moreover, F_L is one of the main observables scanning possible higher twist corrections in the standard Operator Product Expansion (OPE) [8]. Therefore, a reasonable description of this quantity suggests the Glauber-Mueller formalism (or similar eikonal-like approaches) take into account the most important contributions to the complete higher-twist corrections at current kinematical regime.

The structure function $F_2^{c\bar{c}}(x, Q^2)$ gives the charm quark content on the proton and is directly driven by the gluon distribution. Therefore it is a powerful observable to scan saturation effects in the small x region. However the current experimental status requires more dedicated measurements and a better statistics. We verify a consistent description in the rest frame corroborating the similar analysis found in the dipole models [32, 39] and in those ones considering unitarity corrections at laboratory frame [13].

4.1 The Inclusive Structure Function $F_2(x, Q^2)$

Now we perform estimates for the inclusive structure function at the rest frame considering the Glauber-Mueller dipole cross section. The expression for F_2 , with the explicit integration limits on photon momentum fraction z and transverse separation r is,

$$F_2(x, Q^2) = \frac{Q^2}{4\pi^2\alpha_{\text{em}}} \int_0^\infty d^2\mathbf{r} \int_0^1 dz (|\Psi_T(z, \mathbf{r})|^2 + |\Psi_L(z, \mathbf{r})|^2) \sigma_{\text{dipole}}^{GM}(x, \mathbf{r}^2). \quad (4.1)$$

The notation has been introduced in the previous sections. In the Fig. (3) one shows the estimates for the structure function on representative virtualities Q^2 from the latest H1 Collaboration measurements [40]. The longitudinal and transverse contributions are shown separately, being the longitudinal one subdominant as well known. An effective light quark mass (u, d, s quarks) was taken, having the value

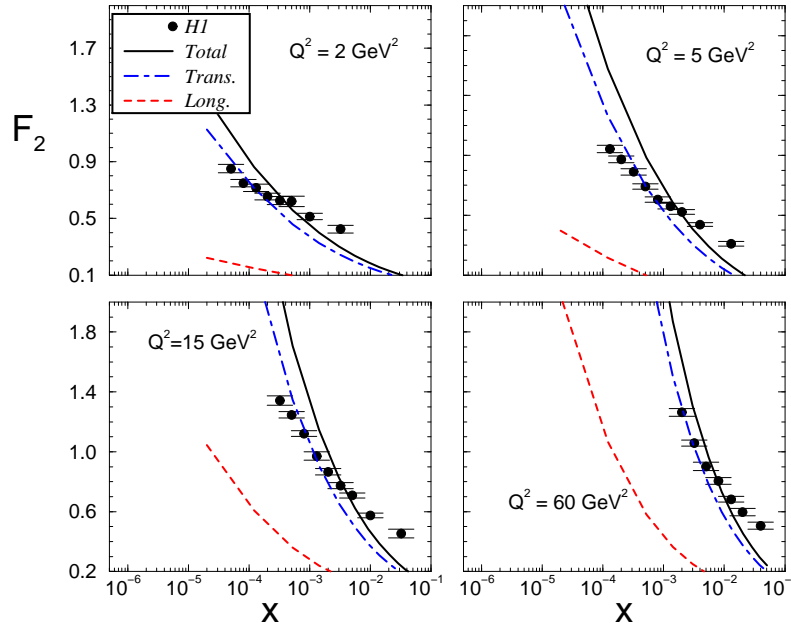


Figure 3: The Glauber-Mueller (GM) result for the $F_2(x, Q^2)$ structure function. It is shown the transverse contribution (dot-dashed), the longitudinal one (dashed) and total one (solid line). One considers light quarks, target radius $R^2 = 5 \text{ GeV}^{-2}$ and frozen gluon distribution at large $r > r_{\text{cut}}$. The input gluon distribution is GRV94LO [37] and data from H1 Collaboration [40].

$m_q = 300 \text{ MeV}$. The target radius is considered $R_A^2 = 5 \text{ GeV}^{-2}$, sound with the studies in Ref. [14]. It should be stressed that this value leads to larger saturation corrections rather than using radius ranging over $R_A^2 \sim 8 - 15 \text{ GeV}^{-2}$. The soft contribution comes from the freezing of the gluon distribution at large transverse separation as discussed at Sec. (2.1). The gluon distribution considered is GRV94 at leading order [37], $xG^{\text{GRV}}(x, \frac{4}{r^2})$, whose choice has been justified in the previous section.

From the plots we verify a good agreement in the normalization, however the slope seems quite steep. This fact is due to the modeling for the soft contribution and it suggests that a more suitable nonperturbative input should be taken. Indeed, in Ref. [34] such a question is addressed, claiming that the correct input is the pion-proton cross section parametrized through the Donnachie-Landshoff pomeron. It is found that the large transverse separations give a larger contribution at low Q^2 , whereas it vanishes concerning higher virtualities.

To clarify this issue, we can calculate the integrand $H_{q\bar{q}}(r, x, Q^2)$ used in the r -integration for the cross section $\sigma_T = \int_0^\infty dr H_{q\bar{q}T}(r, x, Q^2)$. It should have significant nonperturbative content. We plot in the Fig. (4) this quantity at low virtuality $Q^2 = 2 \text{ GeV}^2$ and at higher one $Q^2 = 30 \text{ GeV}^2$ for momentum fraction ranging on $10^{-4} < x < 10^{-2}$. The main contribution comes from an asymmetric peak at

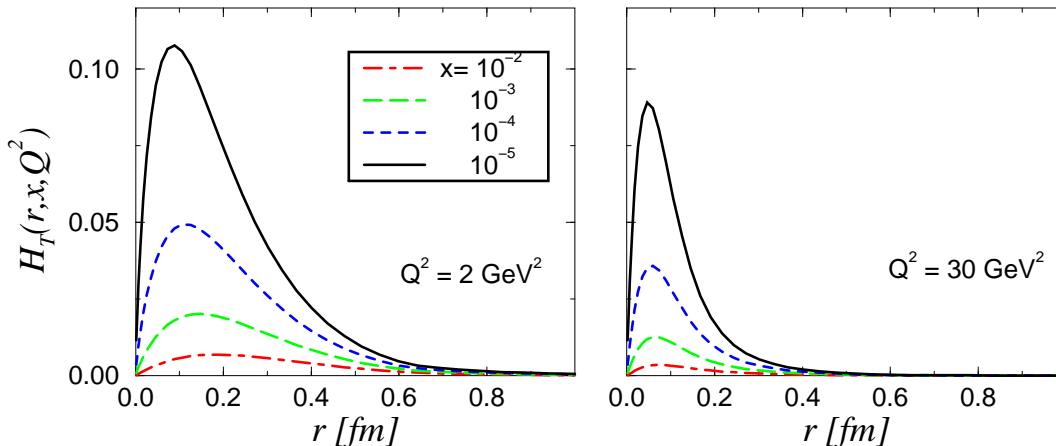


Figure 4: The integrand $H_{q\bar{q}T}(r, x, Q^2)$ as a function of r for $Q^2 = 2$ and $Q^2 = 30$ GeV² at fixed $10^{-5} < x < 10^{-2}$.

$r \approx 0.15$ fm for $Q^2 = 2$ GeV², while it is shifted to $r \approx 0.07$ at $Q^2 = 30$ GeV². In our calculation, the perturbative contribution holds up to $r_{\text{cut}} = 0.62$ fm. Therefore, the region $r > r_{\text{cut}}$ gives a non marginal contribution to the cross section at low virtualities. Indeed, one has found that it reaches about 10 % at $Q^2 = 2$ GeV². As the virtuality increases the contribution gradually vanishes. In fact, using the most recent pdf's this situation is more critical since r_{cut} is smaller ($Q_0^2 \sim 1 - 2$ GeV²). This suggest that the photon piece $|\Psi_T(z, r)|^2$ multiplying the dipole cross section weights the r -integrand to smaller r at high Q^2 . A similar conclusion has already been found in Ref. [34].

To clarify the role played by the soft nonperturbative contribution to the inclusive structure function and to verify the frame invariance of the approach, in the Fig. (5) we plot separately the perturbative contribution and parametrize the soft contribution introducing the nonperturbative structure function $F_2^{\text{soft}} = C_{\text{soft}} x^{-0.08} (1-x)^{10}$, which is summed up to the perturbative one. The soft piece normalization is $C_{\text{soft}} = 0.22$. Such procedure is in order to compare explicitly the results found in Ref. [12]. According, we have used just shadowing corrections for the quark sector, taking into account only the transverse photon wavefunction and zero quark mass. The integration on the transverse separation is taken over $1/Q^2 \leq r^2 \leq 1/Q_0^2$, with $Q_0^2 = 0.4$ GeV² for leading order GRV94 gluon distribution. This leads to a residual contribution to the soft piece coming from transverse separations $r^2 < 1/Q^2$. We considered the target radius being $R_A^2 = 5$ GeV² (supported by [14]), which produces strongest correction rather than a value $R_A^2 = 10$ GeV². It is again verified that the soft contribution is important at small virtualities and decreasing as it is larger. In the plots, the solid lines corresponds to the calculations using the particular approximations indicated above and the dot-dashed ones represents the addition of the soft term.

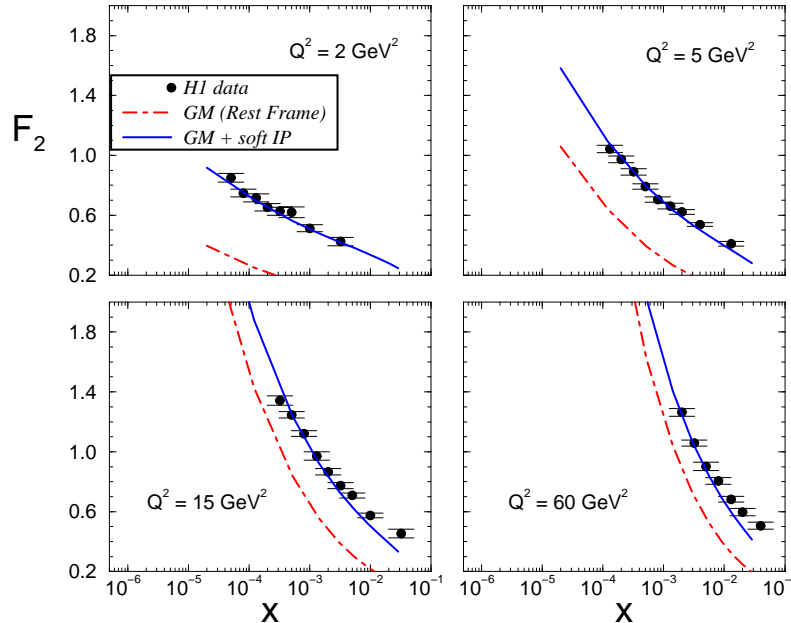


Figure 5: The Glauber-Mueller prediction for the F_2 structure function in the rest frame. For sake of comparison with the results in [12], one uses quark sector ($R^2 = 5 \text{ GeV}^{-2}$, $m_q = 0$) and only transverse wavefunction. The integration limits are $1/Q^2 < r^2 < 1/Q_0^2$ and a soft Pomeron is added (parametrizing the large pair separation - $F_2^{\text{soft}} = C_{\text{soft}} x^{-0.08}(1-x)^{10}$).

Concluding, we have a theoretical estimate, i.e. no fitting procedure, of the inclusive structure function $F_2(x, Q^2)$ through the Glauber-Mueller approach for the dipole cross section, detecting a non negligible importance of a suitable input for the large dipole size region.

4.2 The Logarithmic Slope of $F_2(x, Q^2)$

The global analyzes of the proton structure function data do not present significant deviations from DGLAP approach, however measurements of the rate of change of the logarithmic Q^2 dependence of F_2 , i.e. the Q^2 -slope, have shown possible deviations from the expected pQCD behavior at small x and small Q^2 . These results may be interpreted as signal of unitarity corrections, namely that the system has reached a QCD regime of gluon saturation [7, 14]. Such effects can be analyzed in that quantity, since in leading order DGLAP evolution it is directly proportional to the gluon structure function $xG(x, Q^2)$,

$$\frac{\partial F_2(x, Q^2)}{\partial \ln Q^2} = \frac{2\alpha_s}{9\pi} xG^{\text{DGLAP}}(x, Q^2). \quad (4.2)$$

The most important experimental observation is that at fixed x the slope is a monotonic decreasing function of the virtuality Q^2 . For fixed Q^2 it increases as

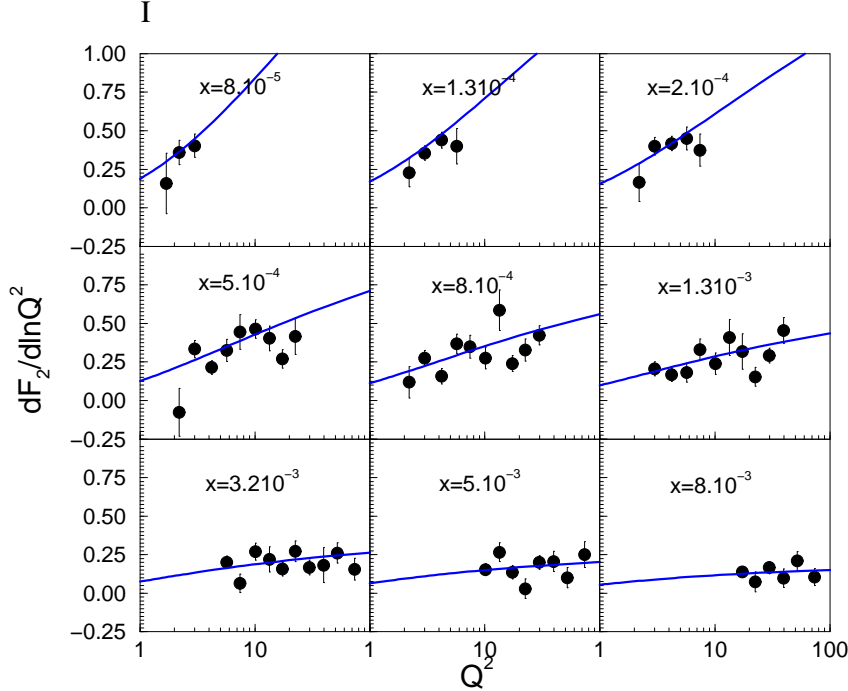


Figure 6: The partial derivative $\partial F_2/\partial \ln Q^2$ plotted as a function of Q^2 (in GeV^2) for fixed x . The solid line corresponds to the Glauber-Mueller prediction. Data from H1 Collaboration [40], where the errors are summed in quadrature.

x becomes smaller. It was verified that the Q^2 -slope behavior as measured in the kinematic region currently available at HERA does not present unambiguous signs of saturation [7]. Indeed, this observable can be described by the usual DGLAP formalism considering the latest parton distribution or DGLAP with saturation effects as well as by some Regge based models. The procedure to distinguish between models for gluon saturation and the Regge inspired ones (including soft and hard interactions) is not an easy task because the saturation scale $Q_s^2(x) \sim 1 - 5 \text{ GeV}^2$ (setting the virtuality where unitarity effects start to be important) at the current HERA domain occurs at similar values of the matching of the soft and hard components. For a similar discussion for the diffractive DIS case, see the Refs. [41].

We can obtain a simple approximation to calculate the logarithmic slope in terms of the dipole cross section. Considering Eqs. (4.2) and (3.10), added of assuming the scale $Q^2 = 4/r^2$ the slope reads as,

$$\frac{\partial F_2(x, Q^2)}{\partial \ln Q^2} = \frac{Q^2}{6\pi^3} \sigma_{q\bar{q}}^{GM}(x, r). \quad (4.3)$$

In the Fig. (6) is shown the result for the expression above in comparison with data on the Q^2 -logarithmic derivative [40], considering the Q^2 dependence at fixed x . A reasonable description is obtained for the measured kinematical range using such an approximation. These results can be comparable with the results [14], where

there is explicit expression for the slope considering unitarity corrections in the quark and gluons sectors. Here, we take into account unitarity effects in the quark sector.

4.3 The Longitudinal Structure Function $F_L(x, Q^2)$

As we saw in the Sec. (2), the inclusive structure function can be expressed in terms of the cross sections σ_T and σ_L for the absorption of virtual photons transversally and longitudinally polarized, $F_2(x, Q^2) = \frac{Q^2}{4\pi\alpha_{\text{em}}}(\sigma_T + \sigma_L)$. At small x , the longitudinal structure function is

$$F_L(x, Q^2) = \frac{Q^2}{4\pi\alpha_{\text{em}}} \sigma_L(x, Q^2). \quad (4.4)$$

From QED, the longitudinal photons have zero helicity ($h = 0$) and therefore they have a virtual character. In the naive parton model, the helicity conservation for the electromagnetic vertex implies to the Callan-Gross relation $F_2 = 2xF_1$ and consequently a vanishing value for the longitudinal structure function $F_L \equiv F_2 - 2xF_1$, considering the scattering photon-quarks (spin 1/2). From QCD theory, the quantity has a non-zero value due to the gluon radiation. This is encoded in the Altarelli-Martinelli expression (see discussion in [13])

$$F_L(x, Q^2) = \frac{\alpha_s(Q^2)}{2\pi} x^2 \int_x^1 \frac{dy}{y^3} \left[\frac{8}{3} F_2(x, Q^2) + \frac{40}{9} y G(y, Q^2) \left(1 - \frac{x}{y} \right) \right], \quad (4.5)$$

where $y = Q^2/sx$ is the inelasticity variable. Therefore, the structure function F_L is an auxiliary observable to detect saturation effects (unitarity corrections) in the gluon distribution.

Experimentally, the determination of the F_L is quite limited, providing few data points. Most recently, the H1 Collaboration has determined the longitudinal structure function through the reduced double differential cross section [40],

$$\sigma_r \equiv F_2(x, Q^2) - \frac{y}{Y_+} F_L(x, Q^2), \quad (4.6)$$

where $Y_+ = 1 + (1 - y)^2$. For large inelasticity, the reduced cross section becomes ($F_2 - F_L$) and the contribution of F_L is enhanced with y^2 . The quantity should be obtained only in the region of large inelasticity, covered in a large range at HERA. In Ref. [40], two methods were used to perform the extraction: (i) for large $Q^2 > 10 \text{ GeV}^2$, F_L is obtained through the "extrapolation method", using a NLO DGLAP QCD fit (in the restrict kinematic range $y < 0.35$ and $Q^2 \leq 3.5 \text{ GeV}^2$) to extrapolate F_2 into the high y region. (ii) At low $Q^2 < 10 \text{ GeV}^2$, the behavior of F_2 as a function of $\ln y$ is obtained using the "derivative method", based on the cross section derivative $(\partial\sigma_r/\partial \ln y)_{Q^2}$. It has found that the first method is more accurate than the derivative one. The data points obtained are consistent with the previous measurements, however they

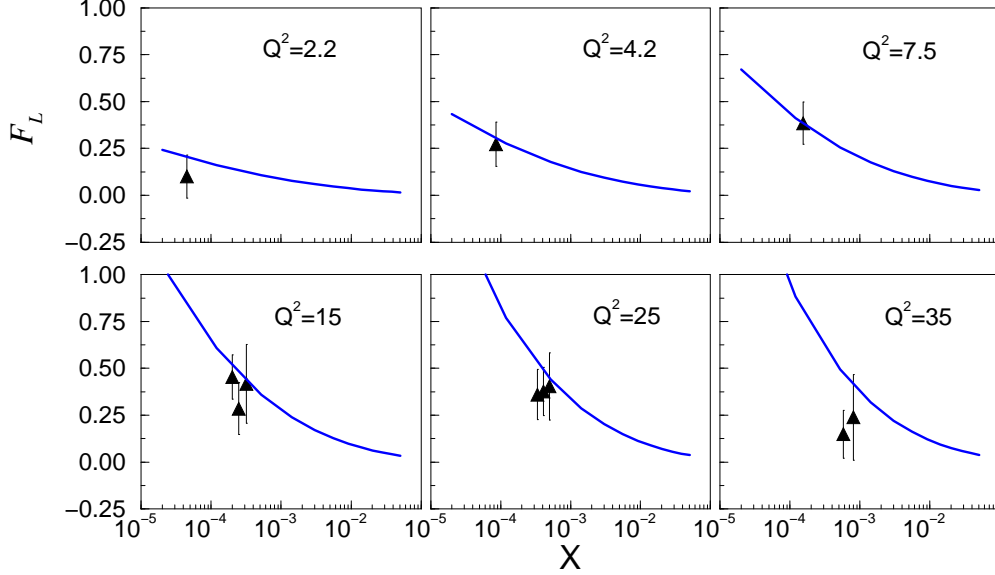


Figure 7: The Glauber-Mueller estimates for the F_L structure function. One uses light quarks ($m_q = 300$ MeV), target size $R^2 = 5$ GeV $^{-2}$ and frozen gluon distribution at large r . Data from H1 Collaboration [40].

are more precise and lying in a broader kinematical range. Therefore, in the following we use only the new data points to analyse.

In Fig. (7) we present the estimates for the F_L structure function, in representative virtualities as a function of x . The previous measured data points have not been included due to their large experimental error bars. In the calculations, it was considered light quarks (u, d, s) with effective mass $m_q = 300$ MeV and the target radius $R^2 = 5$ GeV $^{-2}$. The large r region is considered by the freezing of the gluon distribution at this region. Our expression for the observable is then,

$$F_L(x, Q^2) = \frac{Q^2}{4\pi^2\alpha_{\text{em}}} \int_0^\infty d^2\mathbf{r} \int_0^1 dz |\Psi_L(z, \mathbf{r})|^2 \sigma_{\text{dipole}}^{GM}(x, \mathbf{r}^2). \quad (4.7)$$

The behavior is consistent with the experimental result, either in shape as in normalization. A better description can be obtained by fine tuning the target size or the considered gluon distribution function. Here, it should be stressed the present prediction is parameter-free and determined using the dipole picture taking into account unitarity (saturation) effects in the effective dipole cross section. We verify that the rest frame calculation, taking into account the dipole degrees of freedom and unitarity effects produces similar conclusions to those ones using the

Breit system. For instance, in a previous work [13], the unitarity corrections to the longitudinal structure function were estimated in the laboratory frame considering the Eq. (4.5), with unitarized expressions for F_2 and $xG(x, Q^2)$, obtaining that the expected corrections reaching $\approx 70\%$ as $\ln(1/x) = 15$, namely on the kinematical corner of the upcoming THERA project.

Recently, the higher twist corrections to the longitudinal structure function have been pointed out. For instance, Bartels et al. [8] have calculated numerically the twist-four correction founding they are large for F_T and F_L , however having opposite signs. This fact leads to remaining small effects to the inclusive structure function by almost complete cancellation between those contributions. The higher twist content is analyzed considering the model [33] as initial condition.

Concerning F_L , it was found that the twist-four correction is large and has negative signal, concluding that a leading twist analysis of F_L is unreliable for high Q^2 and not to small x . The results are in agreement with the simple parametrization for higher twist (HT) studied by the MRST group in Ref. [42], where $F_2^{HT}(x, Q^2) = F_2^{LT}(x, Q^2)(1 + \frac{D_2^{HT}(x)}{Q^2})$. The second term would parametrize the higher twist content. In our case, the unitarity corrections provide an important amount of higher twist content, namely it takes into account some of the several graphs determining the twist expansion (for recent discussions in these issues, see [43]).

4.4 The Charm Structure Function $F_2^{c\bar{c}}(x, Q^2)$

In perturbative QCD, the heavy quark production on electron-proton interaction occurs basically through photon-gluon fusion. The emitted photon interacts with a gluon from the proton generating a quark-antiquark pair. Therefore, the heavy quark production allows to determine the gluon distribution and the amount of unitarity (saturation) effects for the observable. In particular, charmed mesons have been measured at deep-inelastic at HERA and the corresponding structure function $F_2^{c\bar{c}}(x, Q^2)$ is defined from the differential cross section for the $c\bar{c}$ pair production,

$$\frac{d^2 \sigma^{c\bar{c}}}{dx dQ^2} = \frac{2\pi\alpha_{em}}{x Q^4} [1 + (1-y)^2] F_2^{c\bar{c}}(x, Q^2), \quad (4.8)$$

with y being the inelasticity variable. In the laboratory frame, the dominant mechanism is the boson-gluon fusion $\gamma^*G \rightarrow c\bar{c}$. Hence, the charm structure function is directly driven by the gluon distribution and provides constraints for the gluonic function. At leading order (LO), it is written as [13],

$$F_2(x, Q^2, m_c^2) = \frac{4\alpha_s(\mu_F^2)}{9\pi} \int_{a_c x}^1 \frac{dy}{y} C_{g,2}^c \left(\frac{x}{y}, \frac{m_c^2}{Q^2} \right) xG(y, \mu_F^2), \quad (4.9)$$

where $a_c = (1 + \frac{m_c^2}{Q^2})$. The mass factorization scale lies in the range $m_c^2 \leq \mu_F^2 \leq 4(Q^2 + 4m_c^2)$. Such a scale introduces an uncertainty of about 10%. An additional

source of uncertainty is the charm mass, in general ranging on $1.2 \leq m_c \leq 1.7$ GeV. The standard QCD coefficient function is labeled by $C_{g,2}^c \left(z, \frac{m_c^2}{Q^2} \right)$.

Experimentally, the latest measurements of the charm structure function are obtained by measuring mesons $D^{*\pm}$ production [44]. For the theoretical input, it was used NLO coefficient functions, considering charm mass $m_c = 1.4$ GeV and factorization-normalization scale $\mu_F = \sqrt{Q^2 + 4m_c^2}$. The function $F_2^{c\bar{c}}(x, Q^2)$ shows a growth with decreasing x at constant values of Q^2 , whereas the rise becomes sharper at higher virtualities. The data are consistent with the NLO DGLAP calculations. Concerning the ratio $R^{c\bar{c}} = F_2^{c\bar{c}}/F_2$, the charm contribution to F_2 grows steeply as x diminishes. It contributes less than 10% at low Q^2 and reaches to about 30 % for $Q^2 > 120$ GeV² [44].

Once more the color dipole picture will provide a quite simple description for the charm structure function in a factorized way. Now, the Glauber-Mueller dipole cross section is weighted by the photon wavefunction constituted by a $c\bar{c}$ pair with mass m_c . Our expression for the charmed contribution in deep inelastic is thus written as

$$F_2^{c\bar{c}}(x, Q^2) = \frac{Q^2}{4\pi^2\alpha_{\text{em}}} \int_0^\infty d^2\mathbf{r} \int_0^1 dz (|\Psi_T^{c\bar{c}}(z, \mathbf{r})|^2 + |\Psi_L^{c\bar{c}}(z, \mathbf{r})|^2) \sigma_{\text{dipole}}^{GM}(x, \mathbf{r}^2) \quad (4.10)$$

where $|\Psi_{T,L}^{c\bar{c}}(z, \mathbf{r})|^2$ is the probability to find in the photon the $c\bar{c}$ color dipole with the charmed quark carrying fraction z of the photon's light-cone momentum with T, L polarizations. For the correspondent wavefunctions, the quark mass in Eqs. (2.10,2.11) should be substituted by the charm quark mass m_c . Here, we should take care of the connection between the Regge parameter $x = (W^2 + Q^2)/(Q^2 + 4m_c^2)$ and the Bjorken variable x_{Bj} . For calculations with the light quarks these variables are equivalent, however for heavier quarks the correct relation is [39],

$$x_{\text{Bj}} = x \left(\frac{Q^2}{Q^2 + 4m_c^2} \right). \quad (4.11)$$

In Fig. (8) we show the estimates for the charm structure function as a function of x_{Bj} [Eq. (4.11)] at representative virtualities. In our calculations, it was used charm mass $m_c = 1.5$ GeV, target size $R^2 = 5$ GeV⁻² and frozen gluon distribution at large r . We have verified small soft contribution, decreasing as the virtuality rises. There is a slight sensitivity to the value for the charm mass, increasing the overall normalization as m_c diminishes. This suggest the charm mass being a scale to suppress the non-perturbative contribution to the corresponding cross section. This conclusion is in agreement with the recent BFKL color dipole calculations of Nikolaev-Zoller [39] and from those ones of Donnachie-Dosch [32].

Regarding the laboratory system description, in Ref. [13] were found strong corrections to the charm structure function, which are larger than of the F_2 ones making use of expression (4.9). Considering the ratio $R_2^c = F_2^{c\text{GM}}(x, Q^2)/F_2^{c\text{DGLAP}}(x, Q^2)$, the corrections predicted by the Glauber-Mueller approach would reach to 62 % at

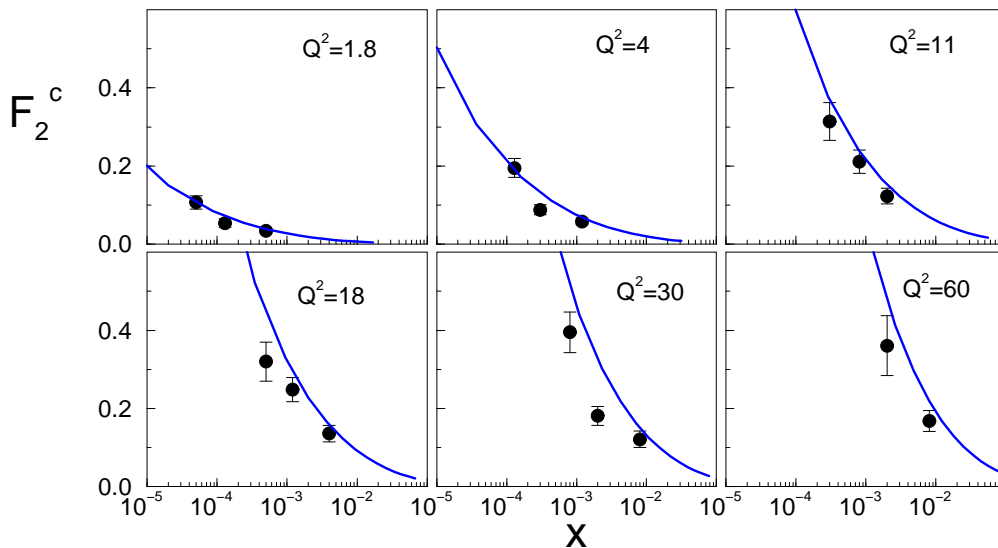


Figure 8: The Glauber-Mueller result for the $F_2^{c\bar{c}}$ structure function as a function of Bjorken variable x . One uses charm mass $m_c = 1.5$ GeV, target size $R^2 = 5$ GeV $^{-2}$ and frozen gluon distribution at large r . Data from ZEUS Collaboration [44] (statistical errors).

values of $\ln(1/x) \approx 15$ (THERA region). There, an important result is large deviation of the standard DGLAP expectations at small x for the ratio $R^{c\bar{c}} = F_2^{c\bar{c}}/F_2$ due to the saturation phenomena (unitarization). With our calculation one verifies that the obtain a good description of data in both reference system, suggesting a consistent estimation of the unitarity effects for the quantity.

5. Conclusions

We study the dipole picture for the description of deep inelastic scattering, focusing on observables driven directly by the gluon distribution. Starting from the dipole cross section provided by the Glauber-Mueller approach in QCD, we perform estimates for the inclusive structure function F_2 , the longitudinal function F_L and the charm structure function on the proton $F_2^{c\bar{c}}$.

For each of the observables above, we obtain parameter-free predictions in good agreement with the updated data from HERA. The resulting calculations corroborate a quite consistent picture for the unitarity corrections from Glauber-Mueller approach in both Breit and rest reference systems. In the laboratory frame the unitarity effects are connected with the gluon distribution function, whereas in the color dipole framework the basic block is the dipole cross section which is corrected by saturation effects.

The small transverse separation r region is dominated by the leading log. DGLAP formalism, with the additional ingredient of unitarization phenomenon as the mo-

momentum fraction acquires quite small values. Such corrections are associated with the taming of the gluon distribution in the very small x region, in general named saturation regime. However, it should be stressed that Glauber-Mueller approach and similar eikonal-like models provide a logarithmic $\ln(1/x)$ asymptotic behavior for the inclusive structure function and gluon distribution, instead a constant value at asymptotic energies.

The large transverse separation is described by non-perturbative aspects of QCD. Since this domain is not well determined at the moment, some modelling of the soft region is needed. In this work we choose the following ansatz: the gluon distribution is frozen for virtualities above a cut radius $r^2 > r_{\text{cut}}^2$, which corresponds to the region $Q^2 < Q_0^2$. A convenient choice for the gluon pdf in order to cover the wider kinematical window possible allows to diminish the uncertainty from the soft sector for the observables. In this order, the most appropriated pdf is the GRV94 parametrization. The value $r_{\text{cut}} = 0.6$ fm is found for that pdf, whereas it can be takes values $r_{\text{cut}} = 0.4 - 0.5$ fm for the more recent pdf's. Throughout the paper we used the target size $R_A^2 = 5 \text{ GeV}^{-2}$, which corresponds to strong unitarity corrections.

When performing a comparison with the phenomenological model GBW, we have found that the Glauber-Mueller approach underestimate the dipole cross section from GBW at not smaller x . Instead, for very low x the Glauber-Mueller overestimates GBW due to the strong increasing of the gluon function at this region. Concerning the saturation model with DGLAP evolution (BGK), it is a particular case of the GM approach when considering central scattering $b = 0$. Despite that the BGK model matches DGLAP evolution, Glauber-Mueller describes properly the realistic impact parameter dependence of the process. Moreover, in GM the extension to the nuclear case is build in.

When considering the structure function F_2 , we have found that it is dominated by small transverse distances contributions. However, a non-negligible content from the soft sector is present. Moreover, the photon wavefunctions weight the dipole cross section into smaller dipole sizes. The weight function selects smaller r as the virtuality Q^2 diminishes. Our estimates here are parameter-free, however a fine tuning of the parameters can improve the data description. We also calculate the F_2 slope in terms of the dipole cross section, which is in agreement with the updated data. Furthermore, we notice that in calculations from [10], only the aligned jet dipole configuration $z, (1 - z) \approx 0$ (and only transverse contribution) is considered, whereas we take into account all configurations, including the symmetric ones. Thus, all dipole sizes, even those from non-perturbative region are included in our results.

Concerning F_L , the estimates are consistent with the previous calculations in the Breit system and are in good agreement with data. A remarkable feature is that the Glauber-Mueller approach in the color dipole framework gives important higher twist contributions to the leading twist calculation in a simple way. As is well known, F_L is the main quantity to study the expected higher twist effects in low virtualities.

The function $F_2^{c\bar{c}}$ is directly dependent of the gluon distribution. Thus, important unitarity correction had been found when considering the Breit frame. Here, we verify consistent results at rest frame in comparison with the previous ones in the fast proton system. We verified that the charm mass suppress soft contributions in comparison with the F_2 case, and the results present a slight dependence with the specific value of m_c .

In conclusion, the Glauber-Mueller approach provides a well established formalism to take into account the unitarity effects. It allows to estimate the higher twist contributions to the quantities in a simplified way. Moreover, it matches DGLAP evolution equation at Born level and includes the impact parameter dependence properly.

Acknowledgments

MVTM acknowledges Martin McDermott (Liverpool University-UK), Igor Ivanov (IKP-Forschungszentrum Juelich, Germany) and Victor Gonçalves (IFM-UFPEL, Brazil) for useful enlightenings. This work was partially financed by CNPq, Brazil.

References

- [1] Yu.L. Dokshitzer. *Sov. Phys. JETP* **46**, 641 (1977);
G. Altarelli and G. Parisi. *Nucl. Phys.* **B126**, 298 (1977);
V.N. Gribov and L.N. Lipatov. *Sov. J. Nucl. Phys* **28**, 822 (1978).
- [2] M.B. Gay Ducati, *Braz. J. Phys.* **31**, 115 (2001), [hep-ph/0107116].
- [3] G.R. Kerley, M. McDermott, *J. Phys.* **G26**, 683 (2000).
M.F. McDermott, Los Alamos preprint [hep-ph/0008260].
- [4] V.N. Gribov. *Sov. Phys. JETP* **29**, 483 (1969).
- [5] N.N. Nikolaev, B.G. Zakharov, *Z. Phys.* **C49**, 607 (1991).
N.N. Nikolaev, B.G. Zakharov, *Phys. Lett.* **B260**, 414 (1991).
N.N. Nikolaev, B.G. Zakharov, *Z. Phys.* **C53**, 331 (1992).
- [6] M. Wüsthoff, *Phys. Rev.* **D56**, 4311 (1997).
- [7] E. Levin, Los Alamos preprint [hep-ph/0105205] (to appear in the THERA book).
- [8] J. Bartels, K.Golec-Biernat, K. Peters. *Eur. Phys. J.* **C17**, 121 (2000).
- [9] A. H. Mueller, *Nucl. Phys.* **B335**, 115 (1990).
- [10] A.L. Ayala, M.B. Gay Ducati and E.M. Levin, *Nucl. Phys.* **B493**, 305 (1997).
A.L. Ayala, M.B. Gay Ducati and E.M. Levin, *Nucl. Phys.* **B511**, 355 (1998).

- [11] L.V. Gribov, E.M. Levin, M.G. Ryskin, *Phys. Rep.* **100**, 1 (1983).
- [12] A.L. Ayala, M.B. Gay Ducati, E.M. Levin, *Eur. Phys. J* **C8**, 115 (1999).
- [13] A.L. Ayala, M.B. Gay Ducati, V.P. Gonçalves, *Phys. Rev.* **D59**, 054010 (1999).
- [14] M.B. Gay Ducati, V.P. Gonçalves, *Phys. Lett.* **B487**, 110 (2000); Erratum-ibid. **B491**, 375 (2000).
- [15] M.B. Gay Ducati, V.P. Gonçalves, *Phys. Rev.* **C60**, 058201 (1999).
M.B. Gay Ducati, V.P. Gonçalves, *Phys. Lett.* **B466**, 375 (1999).
V.P. Gonçalves, *Phys. Lett.* **B495**, 303 (2000).
- [16] M.B. Gay Ducati, V.P. Gonçalves, *Nucl. Phys. (Proc. Suppl.)* **79**, 302 (1999).
M.B. Gay Ducati, V.P. Gonçalves, *Nucl. Phys.* **B557**, 296 (1999).
- [17] A.L. Ayala, M.B. Gay Ducati, E.M. Levin, *Phys. Lett.* **B388**, 188 (1996).
M.B. Gay Ducati, V.P. Gonçalves, *Phys. Lett.* **B502**, 92 (2001).
- [18] E. Gotsman et al., *Phys. Lett.* **B492**, 47 (2000).
E. Gotsman et al., *Nucl. Phys.* **A683**, 383 (2001).
E. Gotsman et al., *Phys. Lett.* **B506**, 289 (2001).
- [19] V. Del Duca, S.J. Brodsky, P. Hoyer, *Phys. Rev.* **D46**, 931 (1992).
- [20] J.R. Forshaw, D.A. Ross. *QCD and the Pomeron*. Cambridge University Press (1997).
- [21] E.A. Kuraev, L.N. Lipatov and V.S. Fadin. *Phys. Lett* **B60** 50 (1975); *Sov. Phys. JETP* **44** 443 (1976); *Sov. Phys. JETP* **45** 199 (1977);
Ya. Balitsky and L.N. Lipatov. *Sov. J. Nucl. Phys.* **28** 822 (1978).
- [22] M.B. Gay Ducati, M.V.T. Machado. *Phys. Rev.* **D63**, 094018 (2001);
M.B. Gay Ducati, M.V.T. Machado. *Nucl. Phys. (Proc. Suppl.)* **B99**, 265 (2001).
M.B. Gay Ducati, M.V.T. Machado. Los Alamos preprint [hep-ph/0104192].
- [23] A. Bialas, H. Navelet, R. Peschanski. *Nucl. Phys.* **B603**, 218 (2001).
- [24] A.V. Lipatov, N.P. Zotov, *Mod. Phys. Lett.* **A15**, 695 (2000).
A.V. Lipatov, V.A. Saleev, N.P. Zotov, *Mod. Phys. Lett.* **A15**, 1727 (2000).
A.V. Kotikov, A.V. Lipatov, G. Parente, N.P. Zotov, Los Alamos preprint [hep-ph/0107135].
- [25] N. Armesto, M.A. Braun, *Eur. Phys. J.* **C20**, 517 (2001).
N. Armesto, M.A. Braun, Los Alamos preprint [hep-ph/0107114].
- [26] I.P. Ivanov, N.N. Nikolaev, *Physics of Atomic Nuclei* **64**, 753 (2001).
- [27] M.A. Kimber, J. Kwiecinski, A.D. Martin, A.M. Stasto, *Phys. Rev.* **D62**, 094006 (2000).
M.A. Kimber, A.D. Martin, M.G. Ryskin, *Phys. Rev.* **D63**, 114027 (2001).

- [28] S. Catani, M. Ciafaloni, F. Hautmann, *Nucl. Phys.* **B366**, 135 (1991).
J.C. Collins, R.K. Ellis, *Nucl. Phys.* **B360**, 3 (1991).
- [29] M. Wusthoff, A.D. Martin. *J. Phys.* **G25**, R309 (1999).
- [30] S. Munier, A.M. Stasto, A.H. Mueller, *Nucl. Phys.* **B603**, 427 (2001).
- [31] J.R. Forshaw, G.R. Kerley, G. Shaw, *Phys. Rev.* **D60**, 074012 (1999).
J.R. Forshaw, G.R. Kerley, G. Shaw, *Nucl. Phys.* **A675**, 80c (2000).
- [32] A. Donnachie, H.G. Dosch, *Phys. Lett.* **B502**, 74 (2001).
A. Donnachie, H.G. Dosch, Los Alamos preprint [hep-ph/0106169]
- [33] K. Golec-Biernat, M. Wüsthoff. *Phys. Rev.* **D59**, 014017 (1999).
K. Golec-Biernat, M. Wüsthoff. *Phys. Rev.* **D60**, 114023 (1999).
- [34] M. McDermott, L. Frankfurt, V. Guzey, M. Strikman, *Eur. Phys. J.* **C16**, 641 (2000).
- [35] E. Gotsman, E. Levin, U. Maor, *Nucl. Phys.* **B493**, 354 (1997).
- [36] A. Kovner, U.A. Wiedemann, *Phys. Rev.* **D64**, 114002 (2001).
- [37] M. Gluck, E. Reya, A. Vogt, *Z. Phys.* **C67**, 433 (1995).
- [38] K. Golec-Biernat, in talk presented at Ringberg Workshop: New Trends in HERA Physics 2001, 17-22 June (2001), [hep-ph/0109010].
H. Kowalski, in talk presented at EPS 2001 Conference, July 12-18, 2001, Budapest, Hungary (2001).
J. Bartels, K. Golec-Biernat, H. Kowalski, (to appear).
- [39] N.N. Nikolaev, V.R. Zoller, *Phys. Lett.* **B509**, 283 (2001).
- [40] H1 Collaboration, *Eur. Phys. J.* **C21**, 33 (2001).
- [41] M.B. Gay Ducati, V.P. Gonçalves, M.V.T. Machado, *Phys. Lett.* **B506**, 52 (2001).
M.B. Gay Ducati, V.P. Gonçalves, M.V.T. Machado, *Nucl. Phys.* **A699**, (2002).
M.B. Gay Ducati, V.P. Gonçalves, M.V.T. Machado, [hep-ph/0110025].
M.B. Gay Ducati, E.G. Ferreira, M.V.T. Machado, C.A. Salgado, [hep-ph/0110184].
- [42] A.D. Martin, R.G. Roberts, W.J. Stirling, R.S. Thorne, *Phys. Lett.* **B443**, 301 (1998);
- [43] E. Gotsman et al., *Phys. Lett.* **B506**, 289 (2001).
E. Gotsman et al., *Nucl. Phys.* **A683**, 283 (2001).
- [44] ZEUS Collaboration, *Eur. Phys. J.* **C12**, 35 (2000).